Contribution from the Department of Chemistry,
University of California, Davis, California 95616

Novel Reactions of Metal–Metal Bonds. Addition of Sulfur Dioxide and Sulfur to $Pd_2(Ph_2PCH_2PPh_2)_2Cl_2$ and the Oxidation of Coordinated Sulfide

ALAN L. BALCH,* LINDA S. BENNER, and MARILYN M. OLMSTEAD

Received March 9, 1979

Sulfur dioxide inserts into the metal–metal bond of $Pd_2(dpm)_2X_2$ (dpm = bis(diphenylphosphino)methane, X = Cl or Br), $Pd_2(dam)_2Cl_2$ (dam = bis(diphenylarsino)methane), and $Pt_2(dpm)_2Cl_2$. The adducts have been crystallized and characterized by infrared, electronic, and ^1H NMR spectroscopy. The structure of $Pd_2(dpm)_2(\mu\text{-}SO_2)Cl_2$ has been determined by X-ray crystallography. The compound crystallizes in the orthorhombic space group $P2_12_12_1$ with four molecules per unit cell of dimensions a = 15.582 (3), b = 16.457 (3), and c = 19.184 (5) Å. Full-matrix least-squares refinement yields R = 0.069. The binuclear molecules contain two approximately planar palladium ions, each coordinated to a terminal chloride, a bridging sulfur dioxide, and two trans phosphorus donors from the bridging diphosphines. The ability of crystal packing forces to alter the Pd···Pd separation (3.383 (4) and 3.220 (4) Å for the two crystallographically independent molecules) reflects the lack of a direct metal–metal bond. $Pd_2(dpm)_2Cl_2$ reacts with *cyclo*-octasulfur or propylene sulfide to give $Pd_2(dpm)_2(\mu\text{-}S)Cl_2$, which has been crystallized and characterized by infrared, electronic, and ^1H NMR spectra. An X-ray structure determination reveals that $Pd_2(dpm)_2(\mu\text{-}S)Cl_2$ has a geometry nearly identical with that of $Pd_2(dpm)_2(\mu\text{-}SO_2)Cl_2$. Crystals of $Pd_2(dpm)_2(\mu\text{-}S)Cl_2$ are tetragonal, space group $P4_1$, with Z = 4 and cell dimensions a = 21.015 (4) and c = 14.281 (2) Å. Refinement of this complex yields an R of 0.076. Oxidation of $Pd_2(dpm)_2(\mu\text{-}S)Cl_2$ with *m*-chloroperbenzoic acid has been monitored by electronic spectroscopy at −60 °C; $Pd_2(dpm)_2(\mu\text{-}SO_2)Cl_2$ is formed. The utility of the ^1H NMR spectra of the methylene region of these dpm-bridged complexes in diagnosing the structure of the complexes is discussed.

Introduction

Palladium(I) and platinum(I) complexes containing direct metal–metal bonds have begun to attract considerable attention.[1-26] Some of these compounds involve unsaturated, four-coordinate metal ions. Unlike the situation with many of the early transition metals, however, these palladium(I) and platinum(I) ions do not form multiple metal–metal bonds with one another. The bond distances in species such as $Pd_2(CNCH_3)_6^{2+}$,[1,2] $Pd_2(dpm)_2Br_2$[11] (dpm = bis(diphenylphosphino)methane), and $Pt_2(dpm)_2Cl_2$[14] indicate that they have only a metal–metal single bond and, as a result, 16 valence electrons. This produces a novel bonding situation in which the metal–metal bond is an unsaturated single bond. In many respects these compounds resemble their much more numerous palladium(II) and platinum(II) counterparts since they display planar coordination and facile ligand substitution reactions.[5]

Of these palladium(I) and platinum(I) species, the unsaturated single bonds of $Pd_2(dpm)_2Cl_2$ and $Pt_2(dpm)_2Cl_2$ display unusual reactivity. Carbon monoxide is readily and reversibly inserted into these metal-metal bonds (eq 1) to yield

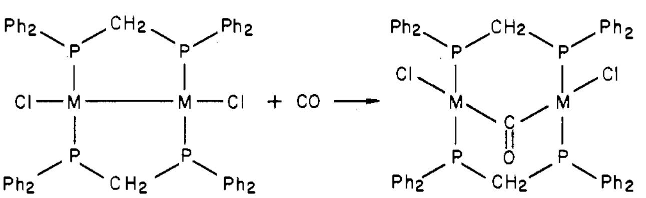

(1)

products in which the metals have moved further apart by about 0.5 Å and are no longer directly bonded.[6,11] Isocyanides[6] and diazonium ions[26] also insert into these metal–metal bonds while nitriles and dinitrogen do not react with $Pd_2(dpm)_2Cl_2$ or $Pt_2(dpm)_2Cl_2$. On the other hand, tin(II) chloride, which is known to insert into some metal–metal bonds, reacts with the Pd–Cl bond rather than the Pd–Pd bond of $Pd_2(dpm)_2Cl_2$ and produces $Pd_2(dpm)_2(SnCl_3)Cl$ and $Pd_2(dpm)_2(SnCl_3)_2$.[8]

This article is a report on our continuing studies of the selectivity of $Pd_2(dpm)_2Cl_2$ and $Pt_2(dpm)_2Cl_2$ toward reaction with small molecules which are known to be reactive toward other metal complexes. We have briefly reported that these complexes reversibly add sulfur dioxide.[7] Details of those reactions are given here. We also report that $Pd_2(dpm)_2Cl_2$ can abstract a sulfur atom from *cyclo*-octasulfur or propylene sulfide to produce a sulfide-bridged species whose skeletal geometry is nearly identical with that of the sulfur dioxide adducts. More surprisingly in terms of reactivity is the observation that $Pd_2(dpm)_2Cl_2$ does not react with dioxygen. Finally we note that the coordinated sulfide in $Pd_2(dpm)_2(\mu\text{-}S)Cl_2$ can be oxidized to coordinated sulfur dioxide.

Experimental Section

Preparation of Compounds. $Pd_2(dpm)_2Cl_2$,[8] $Pd_2(dpm)_2Br_2$,[8] $Pd_2(dam)_2Cl_2$,[8] and $Pt_2(dpm)_2Cl_2$[15] were prepared as described previously. In all cases where complexes are formulated as solvates, the presence of the solvent molecules was verified by ^1H NMR spectroscopy.

$Pd_2(dpm)_2(\mu\text{-}SO_2)Cl_2$. Sulfur dioxide was bubbled into an orange, filtered solution of 0.105 g (0.10 mmol) of $Pd_2(dpm)_2Cl_2$ in 10 mL of dichloromethane for 5 min. Anhydrous methanol (35 mL) was added to the deep violet solution and the mixture was placed in a freezer at −5 °C. The product, which slowly deposited as violet crystals, was collected by filtration, washed with cold methanol, and vacuum dried: yield 85%; mp 180–182 °C. The complex crystallizes with 1 mol of methanol and 0.5 mol of dichloromethane; the ^1H NMR spectrum of the dissolved crystals shows the presence of both methanol and dichloromethane. Anal. Calcd for $C_{50}H_{44}Cl_2O_2P_4Pd_2S\cdot CH_3OH\cdot {}^1/_2CH_2Cl_2$: C, 51.93; H, 4.15; S, 2.69; Cl, 8.93. Found: C, 51.65; H, 4.12; S, 2.71; Cl, 9.02.

$Pd_2(dpm)_2(\mu\text{-}SO_2)Br_2$. This was prepared from $Pd_2(dpm)_2Br_2$ by the method described for $Pd_2(dpm)_2(\mu\text{-}SO_2)Cl_2$. The complex, which forms violet crystals that contain 1 mol of dichloromethane/mol of complex, was obtained in 76% yield: mp 185–187 °C. Anal. Calcd for $C_{50}H_{44}Br_2O_2P_4Pd_2S\cdot CH_2Cl_2$: C, 48.60; H, 3.63; S, 2.58. Found: C, 48.32; H, 3.83; S, 2.58.

$Pd_2(dam)_2(\mu\text{-}SO_2)Cl_2$. This compound was obtained from $Pd_2(dam)_2Cl_2$ via the route described for $Pd_2(dpm)_2(\mu\text{-}SO_2)Cl_2$. It forms violet crystals which contain both methanol and dichloromethane: yield 95%; mp 199 °C. Anal. Calcd for $C_{50}H_{44}As_4Cl_2O_2Pd_2S\cdot {}^1/_2CH_3OH\cdot {}^1/_2CH_2Cl_2$: C, 45.34; H, 3.51; S, 2.37. Found: C, 45.73; H, 3.42; S, 2.27.

$Pt_2(dpm)_2(\mu\text{-}SO_2)Cl_2$. This compound was prepared from $Pt_2(dpm)_2Cl_2$ by the route described for $Pd_2(dpm)_2Cl_2$. It was obtained as bright yellow crystals in 76% yield: mp >250 °C. Anal. Calcd for $C_{50}H_{44}Cl_2O_2P_4Pt_2S\cdot {}^1/_2CH_2Cl_2$: C, 45.39; H, 3.39; S, 2.40. Found: C, 45.44; H, 3.70; S, 1.97.

$Pd_2(dpm)_2(\mu\text{-}S)Cl_2$. Method 1. A mixture of 0.210 g (0.10 mmol) of $Pd_2(dpm)_2Cl_2$ and 0.025 g of sulfur in 15 mL of benzene was heated under reflux for 2 h. The reaction mixture was cooled and hexane was added to complete precipitation of the complex. The yellow-brown solid was recrystallized from dichloromethane/methanol to give the pure crystalline compound in 40% yield.

Method 2. Propylene sulfide (0.10 mL, 1.3 mmol) was added to a solution of 0.303 g (0.288 mmol) of $Pd_2(dpm)_2Cl_2$ dissolved in 25 mL of dichloromethane. The mixture was heated under reflux for

3 h, cooled, filtered, and concentrated to 10 mL under vacuum. The crystalline product was obtained in 55% yield by the addition of methanol to this dichloromethane solution. The products obtained by both methods have identical infrared, electronic, and NMR spectra. Anal. Calcd for $C_{50}H_{44}Cl_2P_4Pd_2S$: C, 55.37; H, 4.09; Cl, 6.54; S, 2.96. Found: C, 54.51; H, 4.21; Cl, 6.95; S, 3.24.

Oxidation of $Pd_2(dpm)_2(\mu\text{-}S)Cl_2$. A 0.4 mM solution of $Pd_2(dpm)_2(\mu\text{-}S)Cl_2$ in dichloromethane, which had been freshly distilled from phosphorus pentoxide, was prepared and then cooled to −60 °C in a liquid nitrogen cooled ethanol bath. A fivefold excess of solid *m*-chloroperbenzoic acid was added to this cold solution. Since the rate of oxidation was slow at this temperature, the solution was removed from the cold bath and allowed to warm slightly. Warming was accompanied by the development of a violet color. Once the intensity of the violet color no longer increased, the solution was returned to the cold bath. The electronic spectral changes accompanying the oxidation are shown in Figure 5.

Physical Measurements. Infrared spectra were recorded on a Perkin-Elmer 180 spectrometer. Electronic spectra were obtained with a Cary 17 spectrophotometer. Measurements at −60 °C were performed by using a Kontes optical Dewar and a bath of ethanol which was cooled by the addition of liquid nitrogen. ^1H NMR spectra (at 100 MHz) and ^{31}P NMR spectra (at 40.5 MHz) were recorded with a JEOL PS-100 pulsed Fourier transform spectrometer. For the ^{31}P NMR spectra, external 85% phosphoric acid was the reference.

X-ray Data Collection. $Pd_2(dpm)_2(\mu\text{-}SO_2)Cl_2\cdot{}^1/_2CH_2Cl_2\cdot CH_3OH$. Crystals were obtained by layering methanol over a dichloromethane solution of $Pd_2(dpm)_2Cl_2$ which had been saturated with sulfur dioxide. A violet needle (0.45 × 0.125 × 0.175 mm), which grew as the components of the mixture diffused together, was selected. Loss of solvent of crystallization was prevented by rapidly mounting the crystal on the goniometer head under a stream of cold nitrogen. Determination of space group, determination of cell dimensions, and intensity data collection were carried out at 150 K, using a Syntex $P2_1$ diffractometer equipped with a graphite monochromator and a Mo X-ray tube ($\lambda(K\alpha)$ 0.710 69 Å). Space group determination followed unambiguously from rotation and axial photographs, coupled with the automatic indexing program of the $P2_1$ software, and from quick scans of the reflections from which systematic absences were expected. Unit cell constants were determined from a least-squares fit of 12 moderately intense reflections in the range $25° < 2\theta < 35°$. A variable-speed (2–60° min^{-1}) ω-scan technique was employed for intensity measurements. A 0.7° scan range and 1° offset for stationary background counts were chosen. The total time for left and right background measurements was 0.5 that spent scanning the peak. The intensities of two standard reflections, recorded every 118 reflections, averaged a random standard deviation of 2.1%. Net intensities were computed from the relationship

$$I = \left(P - \frac{LB + RB}{R}\right) \times SR$$

where *P* is the peak count, LB and RB are left and right background counts, *R* is the ratio of background to scan time, and SR is the scan rate. The standard deviation in intensity is calculated as

$$\sigma(I) = \left(\left[\left(P + \frac{LB + RB}{R}\right)^{1/2} \times SR\right]^2 + (FI)^2\right)^{1/2}$$

where *F* is the average of the standard deviation of check reflections. Of the 3607 reflections that were collected with $2\theta < 45°$, 3220 with $I > 3\sigma(I)$ were used in the final refinement. Intensity data were corrected for Lorentz and polarization effects. For a crystal having the dimensions given, exhibiting a μ of 10.7 cm^{-1}, and mounted along the needle axis, the range of absorption factors is 1.26–1.48, resulting in an error of *F* of <±4%. No absorption correction was applied. Crystal data are reported in Table I.

$Pd_2(dpm)_2(\mu\text{-}S)Cl_2\cdot nCH_2Cl_2$. Crystals were obtained by solvent diffusion of diethyl ether into a dichloromethane solution of the complex. An orange needle measuring 1.0 × 0.12 × 0.13 mm was selected and coated with epoxy resin to prevent loss of occluded solvent. The crystal was then rapidly mounted on the goniometer head under a cold stream of nitrogen vapor. The experimental method for data collection was similar to that for the SO_2-bridged complex. A 4–60° min^{-1} variable-speed ω scan of 1° range was used, with a total background count time equal to that of the peak count time. A check reflection, monitored every 199 reflections, had a random fluctuation of 1.0% during data collection, indicating that solvent loss had been halted. A total of 4600 reflections with $2\theta < 45°$ were measured, of which 4155 had $I > 3\sigma(I)$. Crystal data are summarized in Table I. Intensity data were corrected for Lorentz and polarization effects. For the crystal geometry involved in data collection, absorption factors are 1.27–1.38 resulting in a maximum error of *F* of ±3%. No absorption correction was made.

Table I. Crystal Data for $Pd_2(dpm)_2(\mu\text{-}SO_2)Cl_2$ and $Pd_2(dpm)_2(\mu\text{-}S)Cl_2$

	$Pd_2(dpm)_2(\mu\text{-}SO_2)Cl_2$	$Pd_2(dpm)_2(\mu\text{-}S)Cl_2$
formula	$Pd_2Cl_3SP_4O_3C_{51.5}H_{49}$	$Pd_2Cl_8SP_4C_{53}H_{50}$[a]
formula wt	1191.0	1339.3[a]
a, Å	15.582 (3)	21.015 (4)
b, Å	16.457 (3)	21.015 (4)
c, Å	19.184 (5)	14.281 (2)
V, Å^3	4919.4 (22)	6306.9 (19)
crystal system	orthorhombic	tetragonal
space group	$P2_12_12$ (No. 18)	$P4_1$ (No. 76)
radiation	Mo Kα	Mo Kα
absorption, cm^{-1}	10.7	10.7[a]
Z	4	4
$D_{exptl}(298)$, g cm^{-3}	1.57 (1)	*b*
$D_{calcd}(150)$, g cm^{-3}	1.609	1.41[a]

[a] Assuming three molecules of CH_2Cl_2 per formula unit. [b] Experimental values for density depended on crystal exposure to air and ranged from 1.48 (exposure ca. 1 min) to 1.26 g cm^{-3} (exposure ca. 1 h).

Solution and Refinement of Structures. Both structures were solved by standard Patterson and Fourier techniques and refined by full-matrix least-squares methods. Scattering factors for neutral Pd, P, S, Cl, and C were those of Cromer and Waber[27a] and corrections for the real and imaginary parts of anomalous dispersion for Pd, P, S, and Cl were made.[27b] The crystallographic programs used were developed by H. Hope. Structure drawings were made by using Johnson's ORTEP II.[28] The program used for full-matrix least-squares refinement minimizes the function $\sum w(kF_o - |F_c|)^2$, where *k* is a scale factor and *w* is determined from a Hughes[29] weighting scheme. For the SO_2-bridged structure $4F_{min} = 34.0$ and for the S-bridged structure $4F_{min} = 49.0$. Definitions of the indicators are $R = \sum|F_o - F_c|/\sum|F_o|$ and goodness of fit $= [\sum w(|F_o - |F_c|)^2/(n - m)]^{1/2}$, where *n* is the number of observations and *m* is the number of parameters.

For $Pd_2(dpm)_2(\mu\text{-}SO_2)Cl_2\cdot{}^1/_2CH_2Cl_2\cdot CH_3OH$ all nonhydrogen atoms were found except for the dichloromethane carbon which appeared to be badly disordered. The final refinement was carried out with anisotropic thermal parameters for Pd, S, Cl, and P and isotropic thermal parameters for the remaining nonhydrogen atoms, bringing *R* to 0.069 and R_w to 0.081. Goodness of fit is 0.212 for 215 parameters and the 3220 reflections with $I < 3\sigma(I)$. Final shifts in any parameter were less than $^1/_9$ the corresponding esd. Atomic and thermal parameters and their esd's are listed in Table II. Interatomic distances, interatomic angles, and least-squares planes are given in Tables IV–VI.

With $Pd_2(dpm)_2(\mu\text{-}S)Cl_2$ solution and refinement proceeded similarly. Midway through the solution of the structure we realized that it was isostructural with $Pd_2(dam)_2(\mu\text{-}CO)Cl_2$,[13] but we made no use of this fact except to note that atom positions matched with a 0.5 translation in the anchored *z* coordinate.

In the initial stage of refinement only the real part of the correction for anomalous dispersion was made, and space group $P4_1$ was assumed. Reflections for which $I < 3\sigma(I)$ and $(\sin\theta)/\lambda < 0.2$ were omitted, leaving 3744 reflections. When *R* reached 0.073, the structure factor calculation was carried out for each of the enantiomorphic space groups $P4_1$ and $P4_3$, adding in the imaginary part of the correction for anomalous dispersion for Pd, P, S, and Cl. Of the 3441 reflections with $(\sin\theta)/\lambda > 0.3$ and, 56 were considered to be enantiomer sensitive. The criterion used for selection of enantiomer-sensitive reflections is based upon the function[30]

$$D = (\Delta F_{Bij,c})^2/\sigma^2(F_o)$$

where $F_{Bij,c}$ refers to the Bijvoet difference $F(hkl) - F(\bar{h}\bar{k}\bar{l})$. For the 56 reflections with $D > 4.0$ we obtained $R(P4_1) = 0.0603$ and $R(P4_3) = 0.0649$, indicating that our initial choice of space group was the correct one.

Table II. Final Atomic Fractional Coordinates and Temperature Factors[a] for $Pd_2(dpm)_2(\mu\text{-}SO_2)Cl_2\cdot{}^1/_2CH_2Cl_2\cdot CH_3OH$

Molecule A

atom	x	y	z	B_{11}	B_{22}	B_{33}	B_{12}	B_{13}	B_{23}
Pd(1)	0.09372 (8)	0.05189 (7)	0.15815 (6)	1.97 (5)	1.99 (5)	1.99 (5)	−0.18 (4)	0.05 (4)	−0.05 (4)
Cl(1)	0.20699 (25)	0.10902 (23)	0.09080 (23)	2.26 (16)	2.50 (17)	2.70 (17)	−0.21 (14)	0.11 (14)	−0.12 (14)
S(1)	0.0000	0.0000	0.23425 (27)	2.37 (24)	2.26 (23)	1.82 (21)	−0.06 (20)	0.00	0.00
P(1)	0.15920 (26)	−0.07465 (24)	0.14031 (21)	1.99 (17)	1.90 (16)	2.47 (18)	−0.09 (14)	0.13 (14)	0.23 (14)
P(2)	0.01515 (25)	0.17320 (23)	0.15391 (20)	2.10 (17)	1.61 (15)	2.11 (15)	−0.33 (13)	0.02 (14)	−0.07 (13)

atom	x	y	z	B_{iso}, Å^2	atom	x	y	z	B_{iso}, Å^2
O(1)	0.0400 (7)	−0.0639 (7)	0.2778 (7)	2.8 (2)	C(14)	0.3392 (12)	−0.0686 (11)	0.1490 (9)	3.4 (3)
C(1)	0.1018 (10)	−0.1658 (8)	0.1679 (7)	1.7 (2)	C(15)	0.0194 (10)	0.2203 (10)	0.0679 (8)	2.4 (3)
C(3)	0.1825 (10)	−0.0968 (9)	0.0486 (8)	2.1 (3)	C(16)	0.0185 (11)	0.6185 (10)	0.0104 (8)	2.8 (3)
C(4)	0.2301 (12)	−0.1647 (11)	0.0312 (10)	3.3 (3)	C(17)	0.0173 (11)	0.1991 (10)	−0.0567 (9)	2.7 (3)
C(5)	0.2448 (12)	−0.1849 (12)	−0.0404 (10)	3.7 (4)	C(18)	0.0177 (13)	0.2828 (12)	−0.0671 (10)	4.0 (4)
C(6)	0.2084 (12)	−0.1351 (12)	−0.0913 (10)	3.7 (4)	C(19)	0.0212 (12)	0.3357 (11)	−0.0097 (9)	3.6 (4)
C(7)	0.1616 (12)	−0.0687 (11)	−0.0749 (9)	3.3 (3)	C(20)	0.0204 (11)	0.3053 (10)	0.0582 (9)	2.9 (3)
C(8)	0.1449 (10)	−0.0483 (10)	−0.0042 (8)	2.9 (3)	C(21)	0.0507 (10)	0.2512 (10)	0.2143 (8)	2.5 (3)
C(9)	0.2604 (11)	−0.0833 (10)	0.1853 (9)	3.1 (3)	C(22)	0.1327 (10)	0.2487 (10)	0.2378 (8)	2.5 (3)
C(10)	0.2612 (13)	−0.0988 (12)	0.2563 (10)	3.9 (4)	C(23)	0.1637 (11)	0.3045 (10)	0.2848 (9)	3.1 (3)
C(11)	0.3405 (13)	−0.0996 (12)	0.2918 (10)	4.2 (4)	C(24)	0.1082 (11)	0.3680 (10)	0.3099 (9)	3.0 (3)
C(12)	0.4145 (15)	−0.0882 (13)	0.2551 (11)	4.7 (4)	C(25)	0.0247 (11)	0.3692 (11)	0.2871 (9)	3.2 (3)
C(13)	0.4164 (14)	−0.0726 (12)	0.1873 (11)	4.6 (4)	C(26)	−0.0059 (12)	0.3126 (11)	0.2386 (9)	3.1 (3)

Molecule B

atom	x	y	z	B_{11}	B_{22}	B_{33}	B_{12}	B_{13}	B_{23}
Pd(1)	0.40400 (8)	0.46381 (6)	0.31661 (6)	2.00 (5)	1.84 (4)	1.74 (5)	−0.07 (4)	−0.03 (4)	0.05 (4)
Cl(1)	0.30145 (26)	0.41508 (25)	0.39858 (21)	2.55 (16)	2.79 (18)	2.72 (17)	−0.55 (15)	0.28 (14)	0.18 (14)
S(1)	0.50000	0.50000	0.23536 (27)	2.37 (24)	1.85 (22)	1.82 (21)	1.02 (19)	0.00	0.00
P(1)	0.48169 (26)	0.34205 (23)	0.33632 (21)	2.17 (17)	1.69 (15)	2.28 (16)	0.06 (14)	0.01 (14)	0.17 (13)
P(2)	0.33768 (26)	0.59007 (24)	0.29885 (21)	2.10 (17)	1.76 (16)	2.22 (17)	0.10 (14)	−0.16 (14)	0.03 (13)

atom	x	y	z	B_{iso}, Å^2	atom	x	y	z	B_{iso}, Å^2
O(1)	0.4759 (6)	0.5679 (6)	0.1914 (5)	2.5 (2)	C(14)	0.3922 (11)	0.1933 (9)	0.3518 (8)	2.8 (3)
C(1)	0.4145 (11)	0.6744 (9)	0.2910 (8)	2.3 (3)	C(15)	0.2750 (10)	0.5874 (9)	0.2190 (8)	2.2 (3)
C(3)	0.5125 (10)	0.3245 (10)	0.4268 (8)	2.4 (3)	C(16)	0.2075 (11)	0.5318 (11)	0.2195 (9)	3.2 (3)
C(4)	0.4945 (11)	0.3856 (10)	0.4776 (8)	2.7 (3)	C(17)	0.1526 (12)	0.5226 (11)	0.1602 (10)	3.8 (4)
C(5)	0.5184 (11)	0.3750 (11)	0.5480 (9)	3.0 (3)	C(18)	0.1702 (12)	0.5670 (12)	0.1014 (10)	3.9 (4)
C(6)	0.5620 (12)	0.3038 (11)	0.5662 (10)	3.6 (4)	C(19)	0.2361 (12)	0.6235 (11)	0.0989 (10)	3.5 (3)
C(7)	0.5818 (12)	0.2440 (11)	0.5164 (9)	3.6 (4)	C(20)	0.2917 (11)	0.6350 (10)	0.1596 (9)	3.2 (3)
C(8)	0.5545 (12)	0.2551 (11)	0.4501 (9)	3.4 (4)	C(21)	0.2636 (10)	0.6339 (10)	0.3615 (8)	2.5 (3)
C(9)	0.4207 (10)	0.2546 (9)	0.3074 (8)	2.5 (3)	C(22)	0.2047 (12)	0.6949 (11)	0.3368 (9)	3.4 (3)
C(10)	0.4038 (12)	0.2493 (9)	0.2369 (8)	2.8 (3)	C(23)	0.1572 (13)	0.7397 (12)	0.3867 (10)	4.1 (4)
C(11)	0.3587 (11)	0.1857 (10)	0.2088 (9)	2.9 (3)	C(24)	0.1662 (13)	0.7228 (12)	0.4571 (10)	3.9 (4)
C(12)	0.3288 (12)	0.1222 (11)	0.2534 (9)	3.3 (3)	C(25)	0.2205 (12)	0.6645 (11)	0.4793 (10)	3.8 (4)
C(13)	0.3460 (11)	0.1271 (10)	0.3254 (8)	2.9 (3)	C(26)	0.2720 (12)	0.6167 (11)	0.4340 (9)	3.1 (3)

[a] The anisotropic temperature factor is of the form $\exp[-{}^1/_4(h^2a^{*2}B_{11} + \ldots + klb^*c^*B_{23})]$.

Final refinement was carried out with anisotropic thermal parameters for Pd, P, Cl, and S and the full set of intensity data for which $I > 3\sigma(I)$. Full-matrix least-squares refinement of these 282 parameters converged at an R of 0.076 (4155 reflections) and a goodness of fit 0.459. The last shift in each parameter was less than $^1/_8$ the esd except for x and z of C(16) and C(17), for which it was $^1/_2$ the esd. The large B_{iso} for these two atoms indicates they suffer some disorder. Final fractional coordinates and their esd's are listed in Table III.

A final difference Fourier map revealed solvent peaks that could not easily be assigned to ordered molecules. No effort was made to include them since we felt the title compound was adequately described. Further, this aspect of the structure was expected since crystals of $Pd_2(dpm)_2(\mu\text{-}S)Cl_2$ rapidly lose weight on exposure to air. However, the loss is halted once the crystal is mounted in the cold stream of the diffractometer. For the isostructural $Pd_2(dam)_2(\mu\text{-}CO)Cl_2$, fluid solvent molecules also were found, but since this data set was collected at room temperature, a much greater loss of crystallinity occurred, as indicated by the low intensity of high-angle reflections.

Results

Synthesis and Characterization of the μ-SO_2 and μ-S Complexes. Exposure of an orange dichloromethane solution of $Pd_2(dpm)_2Cl_2$ to sulfur dioxide at 1 atm of pressure causes the solution to acquire a brilliant violet color. From these solutions $Pd_2(dpm)_2(\mu\text{-}SO_2)Cl_2$ has been crystallized (as a solvate containing both methanol and dichloromethane) by the addition of methanol. Similar reactions occur with $Pd_2(dpm)_2Br_2$, $Pd_2(dam)_2Cl_2$, and $Pt_2(dpm)_2Cl_2$, although for the platinum compound the color change is much less striking. The addition of sulfur dioxide is readily reversible for the palladium compounds. In fact, when crystals of $Pd_2(dpm)_2(\mu\text{-}SO_2)Cl_2$ are dissolved in dichloromethane, sulfur dioxide is lost from the complex and $Pd_2(dpm)_2Cl_2$ may be precipitated from solution or it may be converted back into $Pd_2(dpm)_2(\mu\text{-}SO_2)Cl_2$ by reexposure to sulfur dioxide.

Spectroscopic data which characterize these new compounds are contained in Tables VII and VIII. The electronic spectra are particularly useful in monitoring the formation of the sulfur dioxide adducts in solution. The infrared spectra of the solid adducts are dominated by bands due to the diphosphine ligand and these are relatively uninformative for structural characterization. The significant features which differentiate the infrared spectra of the sulfur dioxide adducts from the parent dimers are the presence of additional bands in the regions 1165–1150 and 1041–1025 cm^{-1}, which are due to the symmetric and asymmetric S–O stretching frequencies, respectively, and the increase in the Pd–Cl stretching frequencies in the sulfur dioxide adducts. The S–O stretching frequencies are not in themselves sufficiently characteristic in these or other sulfur dioxide adducts to allow the mode of bonding of the sulfur dioxide to be ascertained.

Table III. Final Atomic Fractional Coordinates and Temperature Factors[a] for $Pd_2(dpm)_2(\mu\text{-}S)Cl_2 \cdot nCH_2Cl_2$

atom	x	y	x	B_{11}	B_{22}	B_{33}	B_{12}	B_{13}	B_{23}
Pd(1)	0.38880 (6)	−0.06939 (7)	0.75000	1.02 (6)	2.02 (6)	1.20 (6)	−0.02 (5)	0.01 (5)	0.11 (5)
Pd(2)	0.28012 (6)	0.01406 (6)	0.85670 (13)	0.99 (6)	1.44 (6)	1.55 (6)	0.01 (5)	−0.02 (5)	0.03 (5)
Cl(1)	0.4557 (2)	−0.0706 (3)	0.6173 (4)	1.62 (19)	5.06 (28)	1.64 (21)	0.33 (19)	0.36 (17)	0.23 (20)
Cl(2)	0.2216 (2)	0.1111 (2)	0.8558 (4)	1.67 (18)	1.66 (18)	2.76 (21)	0.45 (14)	−0.12 (18)	−0.46 (18)
S	0.3290 (2)	−0.0821 (2)	0.8834 (3)	1.68 (19)	1.67 (19)	1.69 (20)	0.15 (15)	0.28 (15)	0.15 (16)
P(1)	0.4647 (2)	−0.0259 (2)	0.8500 (4)	1.21 (19)	2.27 (21)	1.35 (20)	0.19 (16)	−0.13 (17)	0.21 (18)
P(2)	0.3063 (2)	−0.1140 (2)	0.6670 (3)	1.33 (19)	1.44 (19)	1.45 (20)	−0.06 (15)	0.13 (16)	−0.05 (16)
P(3)	0.3642 (2)	0.0619 (2)	0.9356 (4)	1.24 (19)	1.91 (21)	1.57 (20)	−0.22 (16)	−0.10 (16)	0.02 (17)
P(4)	0.2037 (2)	−0.0469 (2)	0.7823 (3)	1.07 (18)	1.15 (18)	1.62 (20)	0.00 (15)	0.09 (16)	0.09 (16)

atom	x	y	z	B_{iso}, Å^2	atom	x	y	z	B_{iso}, Å^2
C(1)	0.4347 (9)	0.0095 (9)	0.9574 (13)	1.5 (3)	C(26)	0.3129 (9)	−0.0108 (9)	0.5456 (15)	2.2 (4)
C(2)	0.2304 (8)	−0.1211 (8)	0.7300 (12)	1.4 (3)	C(27)	0.3449 (10)	0.0894 (10)	1.0532 (15)	2.2 (4)
C(3)	0.5201 (9)	0.0324 (9)	0.8052 (14)	1.7 (3)	C(28)	0.3547 (10)	0.0519 (10)	1.1323 (15)	2.5 (4)
C(4)	0.5070 (10)	0.0628 (10)	0.7217 (14)	2.2 (4)	C(29)	0.3374 (12)	0.0776 (12)	1.2202 (19)	3.8 (5)
C(5)	0.5489 (11)	0.1127 (11)	0.6893 (16)	2.9 (4)	C(30)	0.3071 (11)	0.1379 (11)	1.2286 (17)	3.3 (5)
C(6)	0.6032 (10)	0.1269 (10)	0.7388 (17)	2.8 (4)	C(31)	0.2932 (12)	0.1710 (12)	1.1485 (18)	3.6 (5)
C(7)	0.6159 (11)	0.0948 (11)	0.8203 (17)	3.0 (4)	C(32)	0.3114 (11)	0.1484 (11)	1.0628 (16)	2.9 (4)
C(8)	0.5750 (9)	0.0483 (9)	0.8543 (16)	2.3 (4)	C(33)	0.3887 (9)	0.1313 (9)	0.8801 (14)	1.9 (3)
C(9)	0.5148 (9)	−0.0887 (9)	0.8967 (13)	1.6 (3)	C(34)	0.3755 (10)	0.1538 (10)	0.7935 (15)	2.4 (4)
C(10)	0.5423 (10)	−0.0870 (10)	0.9854 (15)	2.4 (4)	C(35)	0.4036 (11)	0.2090 (11)	0.7527 (17)	3.0 (4)
C(11)	0.5807 (11)	−0.1366 (10)	1.0160 (16)	3.0 (4)	C(36)	0.4551 (10)	0.2371 (10)	0.7909 (16)	2.7 (4)
C(12)	0.5913 (12)	−0.1897 (12)	0.9604 (19)	3.6 (5)	C(37)	0.4763 (12)	0.2163 (12)	0.8777 (19)	3.7 (5)
C(13)	0.5653 (13)	−0.1913 (13)	0.8707 (21)	4.6 (6)	C(38)	0.4503 (10)	0.1636 (10)	0.9249 (16)	2.7 (4)
C(14)	0.5257 (11)	−0.1392 (11)	0.8372 (16)	3.0 (4)	C(39)	0.1451 (8)	−0.0754 (8)	0.8675 (13)	1.4 (3)
C(15)	0.3218 (9)	−0.1978 (9)	0.6288 (14)	2.2 (4)	C(40)	0.1141 (9)	−0.1327 (9)	0.8608 (15)	2.1 (3)
C(16)	0.3789 (30)	−0.2156 (31)	0.5878 (51)	13.4 (18)	C(41)	0.0689 (11)	−0.1512 (11)	0.9282 (16)	2.8 (4)
C(17)	0.3817 (30)	−0.2715 (32)	0.5476 (46)	12.4 (17)	C(42)	0.0553 (10)	−0.1114 (10)	1.0021 (16)	2.6 (4)
C(18)	0.3523 (16)	−0.3215 (16)	0.5842 (25)	5.8 (7)	C(43)	0.0857 (9)	−0.0513 (9)	1.0122 (14)	2.1 (4)
C(19)	0.3042 (13)	−0.3092 (12)	0.6390 (19)	3.9 (5)	C(44)	0.1316 (9)	−0.0351 (9)	0.9430 (14)	2.0 (3)
C(20)	0.2873 (13)	−0.2452 (13)	0.6629 (20)	4.3 (6)	C(45)	0.1584 (8)	−0.0101 (8)	0.6871 (13)	1.4 (3)
C(21)	0.2835 (8)	−0.0716 (8)	0.5609 (13)	1.4 (3)	C(46)	0.1053 (9)	−0.0442 (9)	0.6510 (14)	1.9 (3)
C(22)	0.2344 (8)	−0.0947 (8)	0.5051 (13)	1.5 (3)	C(47)	0.0726 (10)	−0.0198 (10)	0.5730 (14)	2.4 (4)
C(23)	0.2193 (11)	−0.0629 (11)	0.4366 (17)	2.9 (4)	C(48)	0.0911 (9)	0.0365 (10)	0.5346 (15)	2.4 (4)
C(24)	0.2454 (10)	0.0003 (10)	0.4062 (15)	2.6 (4)	C(49)	0.1450 (10)	0.0705 (10)	0.5695 (15)	2.5 (4)
C(25)	0.2921 (9)	0.0245 (9)	0.4645 (14)	1.9 (3)	C(50)	0.1779 (9)	0.0455 (9)	0.6479 (13)	1.6 (3)

[a] The anisotropic temperature factor is of the form $\exp[-{}^1/_4(h^2a^{*2}B_{11} + \ldots + klb^*c^*B_{23})]$.

Table IV. Interatomic Distances for $Pd_2(dpm)_2(\mu\text{-}SO_2)Cl_2$ and $Pd_2(dpm)_2(\mu\text{-}S)Cl_2$ (Å)

	$Pd_2(dpm)_2(\mu\text{-}SO_2)Cl_2$		$Pd_2(dpm)_2$-(μ-S)Cl_2
	molecule A	molecule B	
Pd···Pd	3.383 (4)	3.220 (4)	3.258 (2)
P(1)···P(2)′ [P(3)][a]	3.175 (6)	3.112 (6)	3.059 (7)
P(2)···P(4)			3.058 (7)
Pd(1)–Cl(1)	2.381 (4)	2.381 (4)	2.360 (5)
Pd(2)–Cl(2)			2.383 (5)
Pd(1)–S	2.234 (4)	2.241 (4)	2.298 (5)
Pd(2)–S			2.298 (5)
Pd(1)–P(1)	2.344 (4)	2.372 (4)	2.327 (5)
Pd(1)–P(2)	2.343 (4)	2.345 (4)	2.300 (5)
Pd(2)–P(3)			2.325 (5)
Pd(2)–P(4)			2.312 (5)
S–O	1.48 (1)	1.45 (1)	
P(1)–C(1)	1.82 (1)	1.84 (2)	1.82 (2)
P(3)–C(1)			1.87 (2)
P(2)–C(1)′ [C(2)][a]	1.85 (1)	1.86 (2)	1.84 (2)
P(4)–C(2)			1.82 (2)
P(1)–C(3)	1.83 (2)	1.84 (2)	1.81 (2)
P(1)–C(9)	1.80 (2)	1.81 (2)	1.81 (2)
P(2)–C(15)	1.82 (2)	1.82 (2)	1.87 (2)
P(2)–C(21)	1.82 (2)	1.82 (2)	1.82 (2)
P(3)–C(27)			1.82 (2)
P(3)–C(33)			1.81 (2)
P(4)–C(39)			1.83 (2)
P(4)–C(45)			1.83 (2)

[a] Atom in brackets refers to $Pd_2(dpm)_2(\mu\text{-}S)Cl_2$.

Table V. Interatomic Angles for $Pd_2(dpm)_2(\mu\text{-}SO_2)Cl_2$ and $Pd_2(dpm)_2(\mu\text{-}S)Cl_2$ (deg)

	$Pd_2(dpm)_2(\mu\text{-}SO_2)Cl_2$		$Pd(dpm)_2$-(μ-S)Cl_2
	molecule A	molecule B	
Pd–S–Pd	98.4 (4)	91.9 (4)	90.3 (2)
O–S–O	111.4 (14)	108.9 (14)	
Pd–S–O	111.4 (4)	115.9 (4)	
P(1)–C(1)–P(2)′ [P(3)][a]	119.7 (7)	114.8 (8)	112.0 (10)
P(2)–C(2)–P(4)			113.6 (9)
Cl(2)–Pd(1)–S	171.9 (1)	175.5 (1)	172.1 (2)
Cl(2)–Pd(2)–S			169.9 (2)
P(1)–Pd(1)–P(2)	168.3 (1)	175.3 (1)	173.1 (2)
P(3)–Pd(2)–P(4)			171.9 (2)
P(1)–Pd(1)–Cl(1)	87.1 (1)	87.3 (1)	95.1 (2)
P(2)–Pd(1)–Cl(1)	91.8 (1)	95.7 (1)	91.8 (2)
P(3)–Pd(2)–Cl(2)			91.4 (2)
P(4)–Pd(2)–Cl(2)			96.5 (2)
P(1)–Pd(1)–S	92.3 (1)	89.7 (1)	84.9 (2)
P(2)–Pd(1)–S	90.4 (1)	87.6 (1)	88.2 (2)
P(3)–Pd(2)–S			87.7 (2)
P(4)–Pd(2)–S			84.2 (2)

[a] Atom in brackets refers to $Pd_2(dpm)_2(\mu\text{-}S)Cl_2$.

Refluxing $Pd_2(dpm)_2Cl_2$ with sulfur in benzene solution or with propylene sulfide in dichloromethane solution yields the same product—$Pd_2(dpm)_2(\mu\text{-}S)Cl_2$. This product may be differentiated from $Pd_2(dpm)_2Cl_2$ by its characteristic electronic spectrum. Its infrared spectrum contains both a strong band at 345 cm^{-1} which is absent in the spectrum of $Pd_2(dpm)_2Cl_2$ and, as with $Pd_2(dpm)_2(\mu\text{-}SO_2)Cl_2$, an increased Pd-Cl stretching frequency.

The ^1H NMR spectra of these diphosphine-bridged complexes show, in addition to the low-field multiplet due to the phenyl protons, methylene resonances which are highly informative. Representative spectra in this region are shown in Figure 1. For $Pd_2(dpm)_2Cl_2$ the methylene resonance consists of a quintet.[31] Although for any static structure of the puckered five-membered Pd_2P_2C ring the two methylene protons are inequivalent, motion of the ring should be, and

Table VI. Equations of Least-Squares Planes[a] and Distances of Atoms from These Planes

complex	defining atoms	distances, Å			
$Pd_2(dpm)_2(\mu\text{-}SO_2)Cl_2$, A (plane I)	Pd(I), Cl(1), S, P(1), P(2)	Pd(1)	0.0301	P(1)	−0.2084
		Cl(1)	0.1888	P(2)	−0.2034
		S	0.1935		
$Pd_2(dpm)_2(\mu\text{-}SO_2)Cl_2$, B (plane II)	Pd(1), Cl(1), S, P(1), P(2)	Pd(1)	−0.0043	P(1)	0.0743
		Cl(1)	−0.0668	P(2)	0.0715
		S	−0.0746		
$Pd_2(dpm)_2(\mu\text{-}S)Cl_2$ (plane III)	Pd(1), Cl(1), S, P(1), P(2)	Pd(1)	−0.0685	P(1)	−0.0579
		Cl(1)	0.0877	P(2)	−0.0585
		S	0.0972		
$Pd_2(dpm)_2(\mu\text{-}S)Cl_2$ (plane IV)	Pd(2), Cl(2), S, P(3), P(4)	Pd(2)	−0.0882	P(3)	−0.0735
		Cl(2)	0.1099	P(4)	−0.0726
		S	0.1244		
$Pd_2(dpm)_2(\mu\text{-}SO_2)Cl_2$, A (plane V)	Pd(1), Pd(1)′, S, Cl(1), Cl(1)′	Pd(1)	−0.0299	Cl(1)	0.0137
		Pd(1)′	0.0299	Cl(1)′	−0.0137
		S	0.0000		
$Pd_2(dpm)_2(\mu\text{-}SO_2)Cl_2$, B (plane VI)	Pd(1), Pd(1)′, S, Cl(1), Cl(1)′	Pd(1)	0.0597	Cl(1)	−0.0283
		Pd(1)′	−0.0597	Cl(1)′	0.0283
		S	0.0000		
$Pd_2(dpm)_2(\mu\text{-}S)Cl_2$ (plane VII)	Pd(1), Pd(2), S, Cl(1), Cl(2)	Pd(1)	0.0101	Cl(1)	−0.0040
		Pd(2)	−0.0223	Cl(2)	0.0108
		S	0.0055		

plane I: $8.4708x + 4.100y + 15.3760z - 3.4083 = 0$
plane II: $8.4258x + 6.9855y + 13.9323z - 11.0594 = 0$
plane III: $7.4853x - 19.2088y + 2.7705z - 6.3895 = 0$
plane IV: $-9.5179x - 3.5765y + 12.4980z - 8.0789 = 0$
plane V: $7.6252x + 14.3518y - 10.9885 = 0$
plane VI: $-6.2962x + 15.0536y - 4.3787 = 0$
plane VII: $15.0464x + 9.4767y + 7.6106z - 10.8904 = 0$

[a] Equations have the form $Ax + By + Cz - D = 0$, where x, y, and z are fractional coordinates.

Table VII. Spectroscopic Data for New Compounds

compd	IR, cm^{-1}		electronic spectra
	ν(S–O)	ν(Pd–Cl)	λ_{max}, nm (ϵ_{max}, M^{-1} cm^{-1})
$Pd_2(dpm)_2(\mu\text{-}SO_2)Cl_2$	1028, 1041 1157, 1165	277	511 (7280), 346 sh (16 500)
$Pd_2(dpm)_2(\mu\text{-}SO_2)Br_2$	1025, 1158, 1164		532 (8470), 358 sh (14 300)
$Pd_2(dam)_2(\mu\text{-}SO_2)Cl_2$	1034, 1158, 1168	284	523 (9300), 352 sh (17 600)
$Pt_2(dpm)_2(\mu\text{-}SO_2)Cl_2$	1030, 1150		343 sh (8000)
$Pd_2(dpm)_2(\mu\text{-}S)Cl_2$		288	476 (1410), 327 (19 900), 276 sh (36 700), 253 sh (36 600)
$Pd_2(dpm)_2(\mu\text{-}S)Br_2$			473 (1190), 348 (15 200), 288 sh (35 600), 250 sh (40 700)

Table VIII. NMR Data

compd	$^1H(CH_2)$[a]	^{31}P[b]
$Pd_2(dpm)_2Cl_2$	4.14 ($J_{PH} = 4$)	−3.02
$Pd_2(dam)_2Cl_2$	3.93	
$Pd_2(dpm)_2(\mu\text{-}SO_2)Cl_2$	2.60 ($J_{HH} = 13$, $J_{PH} = 2$), 3.77 ($J_{HH} = 13$, $J_{PH} = 6$)	
$Pd_2(dam)_2(\mu\text{-}SO_2)Cl_2$	2.33, 2.97 ($J_{HH} = 11$) AB quartet	
$Pd_2(dpm)_2(\mu\text{-}S)Cl_2$	2.81 ($J_{HH} = 13$, $J_{PH} = 4$), 4.75 ($J_{HH} = 13$, $J_{PH} = 6$)	5.87
$Rh_2(dpm)_2(\mu\text{-}S)(CO)_2$	3.19 ($J_{HH} = 12$), 5.26 ($J_{HH} = 12$, $J_{PH} = 6$)	
$Pd_2(dam)_2(\mu\text{-}CO)Cl_2$[c]	2.04, 2.48 ($J_{HH} = 11$) AB quartet	

[a] Chemical shifts in parts per million relative to Me_4Si, coupling constants in hertz, solvent $CDCl_3$. [b] Chemical shifts in parts per million relative to 85% H_3PO_4. A positive shift is downfield; solvent $CHCl_3$. [c] Reference 13.

apparently is, sufficient to time average the two proton environments so that only a single chemical shift is observed for these two protons. The multiplet structure arises from coupling to phosphorus. Virtual coupling of ^{31}P nuclei is widely observed in trans disphosphine complexes. This results, for example, in the methyl resonance of $Pd(PMe_2Ph)_2Br_2$ appearing as a 1:2:1 triplet with an apparent P–H coupling constant of 3.5 Hz.[32] For the dinuclear complexes considered here each methylene group resides between two pairs of trans phosphorus atoms. As a result of the strong phosphorus coupling, the ^1H NMR spectrum of the complex AA′A″A‴XX′X″X‴ spin system of $Pd_2(dpm)_2Cl_2$ appears as a deceptively simple quintet with the methylene protons coupled to four apparently equivalent phosphorus nuclei. In the sulfur dioxide bridged complex and the sulfide-bridged

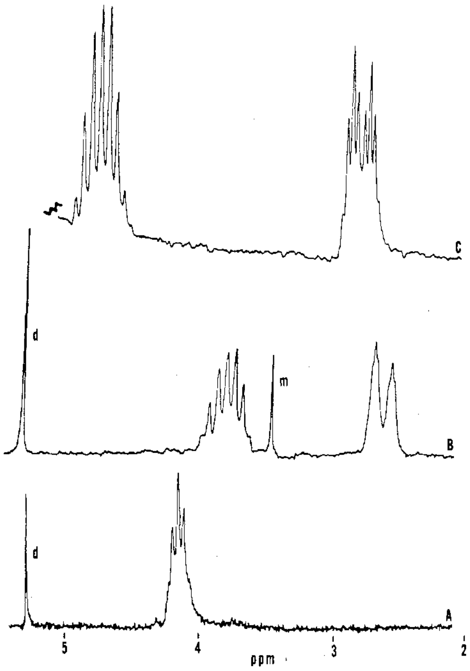

Figure 1. ^1H NMR spectra showing the methylene region of (A) $Pd_2(dpm)_2Cl_2$ in $CDCl_3$, (B) $Pd_2(dpm)_2(\mu\text{-}SO_2)Cl_2$ in $CDCl_3$, and (C) $Pd_2(dpm)_2(\mu\text{-}S)Cl_2$ in CD_2Cl_2. Occluded solvents are indicated by d (dichloromethane) and m (methanol).

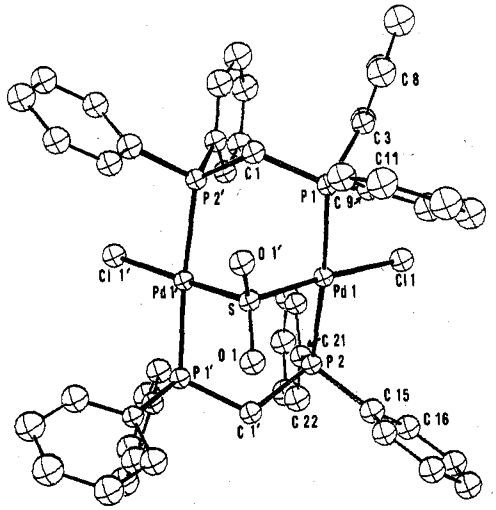

Figure 2. ORTEP drawing of $Pd_2(dpm)_2(\mu\text{-}SO_2)Cl_2$, molecule B, showing 50% thermal ellipsoids.

complex the two methylene protons are no longer equivalent so long as the Pd_2P_2CS ring remains intact. Consequently the methylene resonances of these compounds appear as AB doublets with additional apparent coupling of each methylene proton to four equivalent phosphorus nuclei. In both cases the downfield protons exhibit the larger apparent proton–phosphorus coupling. In Table VIII comparable data are included for $Rh_2(dpm)_2(\mu\text{-}S)(CO)_2$, a bridged species which is isoelectronic with $Pd_2(dpm)_2(\mu\text{-}S)Cl_2$ and possesses a similar structure.[33] Again, for the rhodium compound the methylene region consists of an AB quartet with coupling to four apparently equivalent phosphorus nuclei superimposed.

The methylene protons of the diarsine complexes show similar sensitivity to the nature of the interaction between the metal ions. In $Pd_2(dam)_2Cl_2$ a singlet is observed while in both $Pd_2(dam)_2(\mu\text{-}CO)Cl_2$[13] and $Pd_2(dam)_2(\mu\text{-}SO_2)Cl_2$ quartets are observed because the two protons of each methylene group are no longer able to readily exchange their environments.

Attempts to prepare an oxo-bridged complex analogous to $Pd_2(dpm)_2(\mu\text{-}S)Cl_2$ have revealed the surprisingly inert character of $Pd_2(dpm)_2Cl_2$ when it is treated with molecular oxygen. It has been possible to pass a stream of air through a refluxing benzene solution of $Pd_2(dpm)_2Cl_2$ for 3 h and recover $Pd_2(dpm)_2Cl_2$ in 87% yield from the solution.

Crystal Structures of $Pd_2(dpm)_2(\mu\text{-}SO_2)Cl_2$ and $Pd_2(dpm)_2(\mu\text{-}S)Cl_2$. In order to present a detailed picture of the structures of these compounds, we have determined their X-ray crystal structures. Structural data of this type are particularly important for compounds of this complexity for the following reasons. Complexes of bis(diphenylphosphino)methane show a pronounced tendency to occlude solvent molecules into intermolecular cavities in the solids. The presence of these solvent molecules, combined with incomplete combustion of the dpm ligand, limits the usefulness and reliability of the microanalytical data. Furthermore, spectroscopic probes of changes in the heavy-atom framework of these molecules are generally not available, although now the methylene ^1H NMR resonances can be used to diagnose the nature of the unit bridged by the dpm ligand.

The unit cell of $Pd_2(dpm)_2(\mu\text{-}SO_2)Cl_2$ contains two pairs of crystallographically nonequivalent complex molecules, two molecules of dichloromethane, and four molecules of methanol. There are no unusual intermolecular contacts. An ORTEP drawing of one of the complex molecules—molecule B—is shown in Figure 2. The geometry of the other molecule is similar and a drawing of that molecule is shown in ref 7. Interatomic distances and angles are given in Tables IV and V. Both of these molecules are required by crystal symmetry to have a twofold rotation axis which passes through the sulfur atom and bisects the Pd–Pd and O–O vectors. The palladium ions of both molecules are essentially planar and bonded to four ligand atoms: two phosphorus atoms from the two bridging dpm ligands, the bridging sulfur atom, and the terminal chloride ion. The two coordination planes of the palladium ions meet in a V shape at the bridging sulfur atom. The two palladium ions, the two chloride ligands, and the bridging sulfur atom form another nearly planar group and the P–Pd vectors lie approximately perpendicular to this plane. Equations for the least-squares planes and distances of atoms from these planes are reported in Table VI.

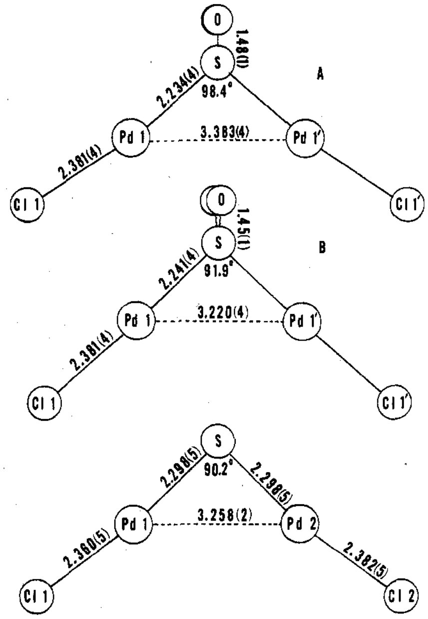

Figure 3. Projection of the Pd, S, O, and Cl atoms in the Pd_2S plane of $Pd_2(dpm)_2(\mu\text{-}SO_2)Cl_2$ and $Pd_2(dpm)_2(\mu\text{-}S)Cl_2$.

There is no Pd–Pd bond in the sulfur dioxide adduct. The Pd–Pd distances in compounds containing Pd–Pd single bonds range from 2.55 to 2.8 Å.[1–3,8,11] In $Pd_2(dpm)_2Br_2$ that distance is 2.669 Å,[11] in $Pd_2(dpm)_2(SnCl_3)Cl$ it is 2.644 Å,[8] and in $Pt_2(dpm)_2Cl_2$ the corresponding Pt–Pt distance is 2.652 Å.[14] The lack of a Pd–Pd bond in the sulfur dioxide bridged dimers is shown not only by the 0.5-Å increase in the Pd–Pd distance but also by the ability of crystal forces to alter this distance significantly (by 0.16 Å) in the two different molecules. Figure 3, a projection of key atoms in the Pd_2S plane, allows a comparison to be made of the major differences (the Pd···Pd separation and the Pd–S–Pd angle) between the two molecules. The two molecules also differ in the degree of planarity of the palladium coordination. In molecule A, the molecule with the larger Pd···Pd separation, the square around each palladium has suffered a diagonal twist toward tetrahedral geometry so that the ligating atoms lie alternately 0.20 Å above and below the least-squares plane of PdP_2SCl. In molecule B the corresponding palladium coordination is less distorted, with all ligating atoms lying within 0.07 Å of the least-squares plane.

$Pd_2(dpm)_2(\mu\text{-}S)Cl_2$ crystallizes with one discrete molecule per asymmetric unit, or four per unit cell; there is no crystallographic symmetry imposed on the molecule. An ORTEP drawing of the molecule is shown in Figure 4. The geometry of this compound is very similar to that of $Pd_2(dpm)_2(\mu\text{-}SO_2)Cl_2$ and $Rh_2(dpm)_2(\mu\text{-}S)(CO)_2$.[33] A comparison of the features in the Pd_2S plane is shown in Figure 3. It is interesting that the sulfur dioxide adduct which readily dissociates possesses shorter Pd–S bonds than does the sulfide-bridged complex from which we have not been able to remove the sulfur. The other differences between molecule A and B of the sulfur dioxide bridged complex are greater than the

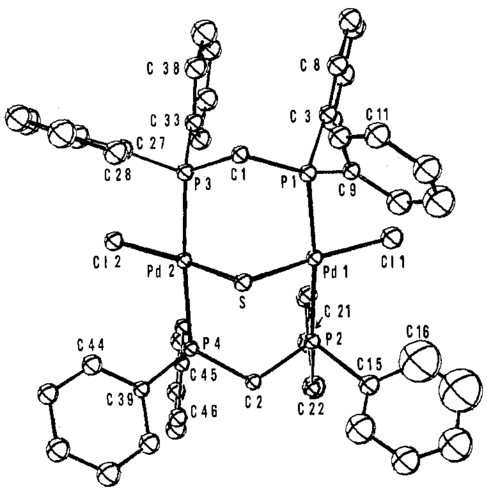

Figure 4. ORTEP drawing of $Pd_2(dpm)_2(\mu\text{-}S)Cl_2$ showing 50% thermal ellipsoids.

differences between molecules of $Pd_2(dpm)_2(\mu\text{-}SO_2)Cl_2$ and $Pd_2(dpm)_2(\mu\text{-}S)Cl_2$. The Rh···Rh separation (3.155 Å) and the Rh–S–Rh bond angle (83.6°) in $Rh_2(dpm)_2(\mu\text{-}S)(CO)_2$ are also comparable to the corresponding distances and angles in $Pd_2(dpm)_2(\mu\text{-}S)Cl_2$. However, the rhodium complex has a geometry which is more twisted than that found in $Pd_2(dpm)_2(\mu\text{-}S)Cl_2$. In the latter complex the Pd–P vectors are nearly perpendicular to the Cl_2Pd_2S plane while in $Rh_2(dpm)_2(\mu\text{-}S)(CO)_2$ the $(OC)_2Rh_2S$ unit is not planar and the diphosphine bridge is twisted. Nevertheless, in these three structures, as in the other A-frame molecules—$Pd_2(dpm)_2(\mu\text{-}CNCH_3)(CNCH_3)_2{}^{2+}$[6] and $Pd_2(dam)_2(\mu\text{-}CO)Cl_2$[12]—the methylene group of the dpm ligands lies over the bridging atom so that the six-membered XM_2P_2C rings have boat rather than chair conformations.

The geometry of $Pd_2(dpm)_2(\mu\text{-}S)Cl_2$ contrasts with that of the Pt(I) sulfide-bridged complex **1**. Unlike the palladium compounds described here, **1** has a short platinum–platinum distance (2.65 Å), which is indicative of the presence of a single bond between the two metal ions and, as a result, a more acute Pt–S–Pt angle (73.1°).[34,35]

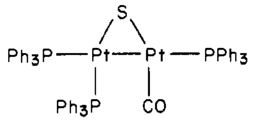

1

Oxidation of the Sulfide Bridge. The structural similarities between $Pd_2(dpm)_2(\mu\text{-}S)Cl_2$ and $Pd_2(dpm)_2(\mu\text{-}SO_2)Cl_2$ suggest that it should be possible to oxidize the bridging sulfide ligand to sulfur dioxide. Peracids have been successfully used to oxidize sulfur atoms in a variety of compounds, including organic disulfides,[36] polysulfides,[37] and cyclic sulfurs,[38] and *m*-chloroperbenzoic acid does oxidize the bridging sulfide of $Pd_2(dpm)_2(\mu\text{-}S)Cl_2$ to sulfur dioxide. This reaction has been monitored by electronic spectra, some of which are reproduced in Figure 5. Traces A and B show the spectra of $Pd_2(dpm)_2(\mu\text{-}S)Cl_2$ and $Pd_2(dpm)_2(\mu\text{-}SO_2)Cl_2$. The sulfur dioxide adduct is unstable in the absence of additional sulfur dioxide, and consequently trace B was obtained from a sulfur dioxide saturated solution. In order to observe the formation of $Pd_2(dpm)_2(\mu\text{-}SO_2)Cl_2$ during oxidation, it is necessary to cool the solution so that the product is stabilized. Trace D shows the spectrum obtained from a mixture of $Pd_2(dpm)_2(\mu\text{-}S)Cl_2$ and *m*-chloroperbenzoic acid at −60 °C. The spectrum recorded indicates the formation of the sulfur dioxide bridged complex. Some additional absorption is present at higher energies and we suspect that this absorption results from further oxidation of the product. Trace C, in which the sulfur dioxide bridged complex is intentionally oxidized, offers some confirmation of this explanation.

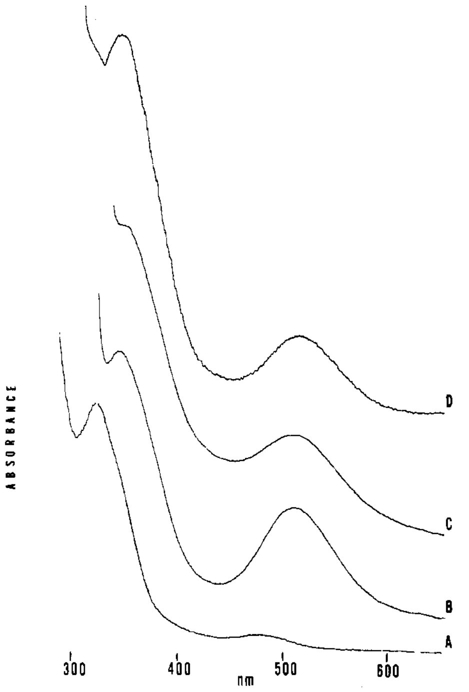

Figure 5. Electronic spectra of 0.4 mM dichloromethane solutions of (A) $Pd_2(dpm)_2(\mu\text{-}S)Cl_2$ at 30 °C, (B) $Pd_2(dpm)_2(\mu\text{-}SO_2)Cl_2$ at −60 °C, (C) $Pd_2(dpm)_2(\mu\text{-}SO_2)Cl_2$ with excess *m*-ClC_6H_4COOOH at −60 °C, and (D) $Pd_2(dpm)_2(\mu\text{-}S)Cl_2$ with excess *m*-ClC_6H_4COOOH at −60 °C.

Scheme I

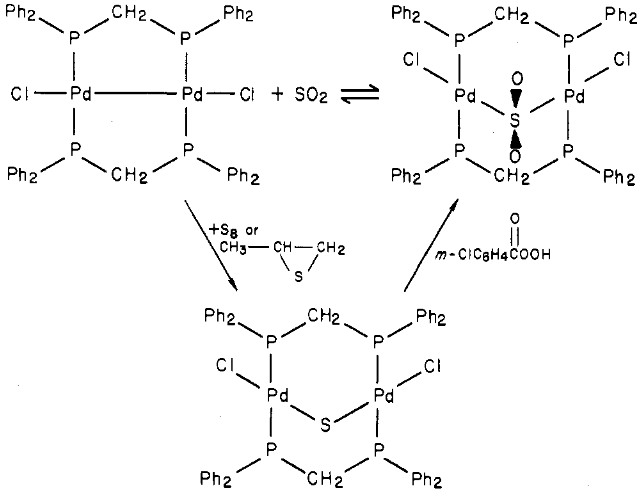

The oxidation of the bridging sulfide by *m*-chloroperbenzoic acid should be a stepwise process with $Pd_2(dpm)_2(\mu\text{-}SO)Cl_2$ as an intermediate. Attempts to isolate a product at room temperature from the reaction of $Pd_2(dpm)_2(\mu\text{-}S)Cl_2$ and *m*-chloroperbenzoic acid carried out with strictly 1:1 stoichiometry have yielded mixtures of unidentified materials, and we suspect that any intermediates in this oxidation have a lower stability than does $Pd_2(dpm)_2(\mu\text{-}SO_2)Cl_2$.

Discussion

The reactions described here are summarized in Scheme I. The addition of sulfur dioxide reported here is the first structurally characterized case of sulfur dioxide insertion into a metal–metal bond and the only reversible case known. The most closely related example is the reaction of $M_2(CO)_{10}{}^{2-}$ (M = Cr, Mo) with sulfur dioxide which is believed to form

$(CO)_5MSO_2M(CO)_5^{2-}$.[39] Other cases of sulfur dioxide bridging two metals are known, but the mode of formation is different from that used to make $Pd_2(dpm)_2(\mu\text{-}SO_2)Cl_2$. Structurally characterized molecules which have sulfur dioxide bridging two bonded metal atoms include $Fe_2(CO)_8(\mu\text{-}SO_2)$,[40] $Ir_2(CO)_4(PPh_3)_2(\mu\text{-}SO_2)$,[41] $(\eta^5\text{-}C_5H_5)_2Fe_2(CO)_2(\mu\text{-}CO)(\mu\text{-}SO_2)$,[42] and $(t\text{-}BuNC)_5Pd_3(\mu\text{-}SO_2)_2$.[43] $(\eta^5\text{-}C_5H_5)_2Fe_2(CO)_4(\mu\text{-}SO_2)$[44] is the only other structurally characterized example of two nonbonded metal ions bridged by sulfur dioxide.

In addition to these bridging modes of coordination, sulfur dioxide can bind a single metal ion in three other forms: η^1-planar, η^1-pyramidal, and η^2.[45] While the infrared spectra in the region of ν(S–O) are indicative of either η^1-planar bonding when the two S–O stretching vibrations occur at ca. 1300 and 1100 cm^{-1} or η^2 bonding when the lower frequency occurs at very low energies (948–895 cm^{-1}),[47] there is about a 200-cm^{-1} difference between the two S–O stretching frequencies; the other three classes of sulfur dioxide coordination have ν(S–O) in the regions 1223–1135 and 1053–993 cm^{-1} [45] and no characteristics have emerged which allow these structural types to be distinguished.

A number of reactions of *cyclo*-octasulfur with transition-metal complexes have been characterized. With $(CF_3)_2C_2S_2Fe_2(CO)_6$ or $(\eta^5\text{-}C_5H_5)_2Fe_2(CO)_4$, the products $[(CF_3)_2C_2S_2FeS]_4$[48] and $[(\eta^5\text{-}C_5H_5)FeS]_4$[49] contain bridging sulfide ions. Under other conditions the *cyclo*-octasulfur/$(\eta^5\text{-}C_5H_5)_2Fe_2(CO)_4$ reaction can produce S_2 ligands.[50] Similarly $(Ph_2PCH_2CH_2PPh_2)_2Ir^+$ reacts with sulfur to give $(Ph_2PCH_2CH_2PPh_2)_2IrS_2^+$.[51] In another reaction type $(\eta^5\text{-}C_5H_5)_2TiCl_2$ reacts with *cyclo*-octasulfur under photolysis to give $(\eta^5\text{-}C_5H_5)_2TiS_5$.[52]

Despite the number of sulfide-bridged structures which are known in transition-metal complexes, this work represents the first example of an oxidation of coordinated sulfide. However, other types of coordinated sulfur have been oxidized. The oxidation of coordinated thiols to S-bonded sulfinate ligands has been known for some time.[53,54] Recently the oxidation of a coordinated thiol has been interrupted so that an S-bound sulfenato ligand was produced.[55] Coordinated disulfur in $(Ph_2PCH_2CH_2PPh_2)_2IrS_2^+$ has also been oxidized to produce both $(Ph_2PCH_2CH_2PPh_2)_2IrS_2O^+$ and $(Ph_2PCH_2CH_2PPh_2)_2IrS_2O_2^{2+}$.[56,57] From the diversity of these examples it appears that the oxidation of coordinated sulfur in its numerous forms should be common and that other attempts of such oxidations will be successful.

Acknowledgment. We thank the National Science Foundation for support, Professor H. Hope for assistance with the crystallography, and Dr. R. Colton for sparking our interest in the methylene ^1H NMR resonances of dpm and a preprint of ref 13. Acquisition of the diffractometer used in this study was made possible through an NSF instrument grant.

Registry No. $Pd_2(dpm)_2(\mu\text{-}SO_2)Cl_2\cdot CH_3OH\cdot{}^1/_2CH_2Cl_2$, 67414-87-3; $Pd_2(dpm)_2(\mu\text{-}SO_2)Br_2$, 71230-19-8; $Pd_2(dam)_2(\mu\text{-}SO_2)Cl_2$, 71171-28-3; $Pt_2(dpm)_2(\mu\text{-}SO_2)Cl_2$, 68851-13-8; $Pd_2(dpm)_2(\mu\text{-}S)Cl_2\cdot 3CH_2Cl_2$, 71277-75-3; $Pd_2(dpm)_2Cl_2$, 64345-29-5; $Pd_2(dpm)_2Br_2$, 60482-68-0; $Pd_2(dam)_2Cl_2$, 67415-28-5; $Pt_2(dpm)_2Cl_2$, 61250-65-5; $Pd_2(dpm)_2(\mu\text{-}S)Br_2$, 71230-61-0; $Rh_2(dpm)_2(\mu\text{-}S)(CO)_2$, 64424-95-9.

Supplementary Material Available: Structure factor tables for $Pd_2(Ph_2PCH_2PPh_2)_2(\mu\text{-}S)Cl_2$ and $Pd_2(Ph_2PCH_2PPh_2)_2(\mu\text{-}SO_2)Cl_2\cdot{}^1/_2CH_2Cl_2\cdot CH_3OH$ (47 pages). Ordering information is given on any current masthead page.

References and Notes

(1) D. J. Doonan, A. L. Balch, S. Z. Goldberg, R. Eisenberg, and J. S. Miller, *J. Am. Chem. Soc.*, **97**, 1961 (1975).
(2) S. Z. Goldberg and R. Eisenberg, *Inorg. Chem.*, **15**, 535 (1976).
(3) A. L. Balch, J. R. Boehm, H. Hope, and M. M. Olmstead, *J. Am. Chem. Soc.*, **98**, 7431 (1976).
(4) J. R. Boehm, D. J. Doonan, and A. L. Balch, *J. Am. Chem. Soc.*, **98**, 4845 (1976).
(5) J. R. Boehm and A. L. Balch, *Inorg. Chem.*, **16**, 778 (1977).
(6) M. M. Olmstead, H. Hope, L. S. Benner, and A. L. Balch, *J. Am. Chem. Soc.*, **99**, 5502 (1977).
(7) L. S. Benner, M. M. Olmstead, H. Hope, and A. L. Balch, *J. Organomet. Chem.*, **153**, C31 (1978).
(8) M. M. Olmstead, L. S. Benner, H. Hope, and A. L. Balch, *Inorg. Chim. Acta*, in press.
(9) L. S. Benner and A. L. Balch, *J. Am. Chem. Soc.*, **100**, 6099 (1978).
(10) R. Colton, R. H. Farthing, and M. J. McCormick, *Aust. J. Chem.*, **26**, 2607 (1973).
(11) R. G. Holloway, B. R. Penfold, R. Colton, and M. M. McCormick, *J. Chem. Soc., Chem. Commun.*, 485 (1976).
(12) R. Colton, M. J. McCormick, and C. D. Pannan, *J. Chem. Soc., Chem. Commun.*, 823 (1977).
(13) R. Colton, M. J. McCormick, and C. D. Pannan, *Aust. J. Chem.*, **31**, 1425 (1978).
(14) M. P. Brown, R. J. Puddephatt, M. Rashidi, and K. R. Seddon, *Inorg. Chim. Acta*, **23**, L33 (1977).
(15) M. P. Brown, R. J. Puddephatt, M. Rashidi, and K. R. Seddon, *J. Chem. Soc., Dalton Trans.*, 951 (1977).
(16) M. P. Brown, R. J. Puddephatt, M. Rashidi, and K. R. Seddon, *Inorg. Chim. Acta*, **23**, L27 (1977).
(17) F. Glockling and R. J. I. Pollock, *J. Chem. Soc., Dalton Trans.*, 2259 (1974).
(18) M. F. Rettig, E. A. Kirk, and P. M. Matlis, *J. Organomet. Chem.*, **111**, 113 (1976).
(19) A. Modinos and P. Woodward, *J. Chem. Soc., Dalton Trans.*, 1516 (1975).
(20) P. L. Goggin and R. J. Goodfellow, *J. Chem. Soc., Dalton Trans.*, 2355 (1973).
(21) P. L. Goggin and J. Mink, *J. Chem. Soc., Dalton Trans.*, 534 (1974).
(22) J. R. Jack, C. J. May, and J. Powell, *J. Am. Chem. Soc.*, **99**, 4707 (1977).
(23) A. Ducruix, H. Felkin, C. Pascard, and G. K. Turner, *J. Chem. Soc., Chem. Commun.*, 615 (1975).
(24) H. Felkin and G. K. Turner, *J. Organomet. Chem.*, **129**, 429 (1977).
(25) H. Werner, A. Kühn, and D. J. Tune, *Chem. Ber.*, **110**, 1763 (1977).
(26) A. D. Rattray and D. Sutton, *Inorg. Chim. Acta*, **27**, L85 (1978).
(27) "International Tables for X-Ray Crystallography", Vol. IV, Kynoch Press, Birmingham, England, 1974: (a) pp 99–101; (b) pp 149–50.
(28) C. K. Johnson, "ORTEP: A Fortran Thermal-Ellipsoid Plot Program for Crystal Structure Illustrations", Report ORNL-3794 (2nd revision), Oak Ridge National Laboratory, Oak Ridge, Tenn., 1970.
(29) E. W. Hughes, *J. Am. Chem. Soc.*, **63**, 1737 (1941).
(30) H. Hope and U. de la Camp, *Acta Crystallogr., Sect. A*, **28**, 201 (1972).
(31) The spectrum of $Pd_2(dpm)_2Cl_2$ reproduced in Figure 1 differs from that reported in ref 13. We have obtained identical spectra from several independent preparations. The additional lines seen in the spectrum shown in ref 13 must arise from impurities.
(32) J. M. Jenkins and B. L. Shaw, *J. Chem. Soc. A*, 770 (1966).
(33) C. P. Kubiak and R. Eisenberg, *J. Am. Chem. Soc.*, **99**, 6129 (1977).
(34) A. C. Skapski and P. G. H. Troughton, *J. Chem. Soc., Chem. Commun.*, 170 (1969).
(35) M. C. Baird and G. Wilkinson, *J. Chem. Soc. A*, 865 (1967).
(36) W. L. Savige and L. A. MacLaren in "Organic Sulfur Chemistry", Vol. 2, N. Kharash, Ed., Pergamon Press, Oxford, 1966, p 367.
(37) R. Steudel and J. Latte, *Chem. Ber.*, **110**, 423 (1977).
(38) R. Steudel and T. Sandow, *Angew. Chem., Int. Ed. Engl.*, **15**, 773 (1976).
(39) J. K. Ruff, *Inorg. Chem.*, **6**, 2080 (1967).
(40) J. Meunier-Piret, P. Piret, and M. van Meersche, *Bull. Soc. Chim. Belg.*, **76**, 374 (1967).
(41) M. Angoletta, P. L. Bellon, M. Manassero, and M. Sansori, *J. Rganomet. Chem.*, **81**, C40 (1974).
(42) M. R. Churchill and K. L. Kalra, *Inorg. Chem.*, **12**, 1650 (1973).
(43) S. Otsuka, Y. Tatsuno, M. Miki, T. Aoki, M. Matsumoto, H. Yoshioka, and K. Nakatsu, *J. Chem. Soc., Chem. Commun.*, 445 (1973).
(44) M. R. Churchill, B. G. DeBoer, K. L. Kalra, P. Reich-Rohrwig, and A. Wojcicki, *J. Chem. Soc., Chem. Commun.*, 981 (1972); M. R. Churchill, B. G. DeBoer, and K. L. Kalra, *Inorg. Chem.*, **12**, 1646 (1973).
(45) For a review on platinum metal complexes of sulfur dioxide see D. M. P. Mingos, *Transition Met. Chim.*, **3**, 1 (1978).
(46) G. J. Kubas, Abstracts, 172nd National Meeting of the American Chemical Society, San Francisco, Calif., September 1976; Abstract No. 240.
(47) R. D. Wilson and J. A. Ibers, *Inorg. Chem.*, **17**, 2134 (1978).
(48) A. L. Balch, *J. Am. Chem. Soc.*, **91**, 6962 (1969).
(49) R. A. Schunn, C. S. Fritchie, and C. T. Prewitt, *Inorg. Chem.*, **5**, 892 (1966).
(50) C. Giannotti, A. M. Ducourant, H. Chanaud, A. Chiaroni, and C. Riche, *J. Organomet. Chem.*, **140**, 289 (1977).
(51) A. P. Ginsberg and W. E. Lindsell, *J. Chem. Soc., Chem. Commun.*, 232 (1971).
(52) E. F. Epstein, I. Bernal, and H. Knopfi, *J. Organomet. Chem.*, **26**, 229 (1971).
(53) M. P. Schubert, *J. Am. Chem. Soc.*, **55**, 3336 (1933).
(54) B. A. Lange, K. Libson, E. Deutsch, and R. C. Elder, *Inorg. Chem.*, **15**, 2985 (1976).
(55) C. P. Sloan and J. H. Krueger, *Inorg. Chem.*, **14**, 1481 (1975).
(56) G. Schmid and G. Ritter, *Chem. Ber.*, **108**, 3008 (1975).
(57) G. Schmid and G. Ritter, *Angew. Chem., Int. Ed. Engl.*, **14**, 645 (1975).